



HAL
open science

Accurate protein-peptide titration experiments by nuclear magnetic resonance using low-volume samples

Christian Kohler, Raphaël Recht, Marc Quinternet, Frédéric de Lamotte,
Marc-André Delsuc, Bruno Kieffer

► To cite this version:

Christian Kohler, Raphaël Recht, Marc Quinternet, Frédéric de Lamotte, Marc-André Delsuc, et al.. Accurate protein-peptide titration experiments by nuclear magnetic resonance using low-volume samples. *Affinity Chromatography: Methods and Protocols*, 1286, Humana Press, 341 p., 2015, *Methods in Molecular Biology*, 978-1-4939-2447-9. 10.1007/978-1-4939-2447-9_22 . hal-02801062

HAL Id: hal-02801062

<https://hal.inrae.fr/hal-02801062v1>

Submitted on 5 Jun 2020

HAL is a multi-disciplinary open access archive for the deposit and dissemination of scientific research documents, whether they are published or not. The documents may come from teaching and research institutions in France or abroad, or from public or private research centers.

L'archive ouverte pluridisciplinaire **HAL**, est destinée au dépôt et à la diffusion de documents scientifiques de niveau recherche, publiés ou non, émanant des établissements d'enseignement et de recherche français ou étrangers, des laboratoires publics ou privés.

Metadata of the chapter that will be visualized online

Chapter Title	Accurate Protein–Peptide Titration Experiments by Nuclear Magnetic Resonance Using Low-Volume Samples
Copyright Year	2015
Copyright Holder	Springer Science+Business Media New York
Author	Family Name Köhler Particle Given Name Christian Suffix Organization Institut de Génétique et de Biologie Moléculaire et Cellulaire Address 1, rue Laurent Fries, BP 1014267404 Illkirch Cedex, France
Author	Family Name Recht Particle Given Name Raphaël Suffix Organization Institut de Génétique et de Biologie Moléculaire et Cellulaire Address 1, rue Laurent Fries, BP 1014267404 Illkirch Cedex, France
Author	Family Name Quinternet Particle Given Name Marc Suffix Division FR CNRS-3209 Bioingénierie Moléculaire, Cellulaire et Thérapeutique (BMCT) Organization CNRS, Université de Lorraine Address Biopôle, Campus Biologie Santé, CS 5018454505 Vandœuvre-lès-Nancy Cedex, France
Author	Family Name Lamotte Particle de Given Name Frederic Suffix Organization INRA, UMR AGAP Address 34398 Montpellier Cedex 5, France
Author	Family Name Delsuc Particle Given Name Marc-André Suffix Organization Institut de Génétique et de Biologie Moléculaire et Cellulaire Address 1, rue Laurent Fries, BP 1014267404 Illkirch Cedex, France

Corresponding Author	Family Name	Kieffer
	Particle	
	Given Name	Bruno
	Suffix	
	Organization	Institut de Génétique et de Biologie Moléculaire et Cellulaire
	Address	1, rue Laurent Fries, BP 1014267404 Illkirch Cedex, France
	Email	kieffer@igbmc.fr

Abstract NMR spectroscopy allows measurements of very accurate values of equilibrium dissociation constants using chemical shift perturbation methods, provided that the concentrations of the binding partners are known with high precision and accuracy. The accuracy and precision of these experiments are improved if performed using individual capillary tubes, a method enabling full automation of the measurement. We provide here a protocol to set up and perform these experiments as well as a robust method to measure peptide concentrations using tryptophan as an internal standard.

Keywords (separated by '-') Affinity measurements - Protein-peptide interactions - NMR - Equilibrium binding constants

Accurate Protein–Peptide Titration Experiments by Nuclear Magnetic Resonance Using Low-Volume Samples 2 3

Christian Köhler, Raphaël Recht, Marc Quinternet, Frederic de Lamotte, 4 [AU1](#)
Marc-André Delsuc, and Bruno Kieffer 5

Abstract 6

NMR spectroscopy allows measurements of very accurate values of equilibrium dissociation constants using 7
chemical shift perturbation methods, provided that the concentrations of the binding partners are known 8
with high precision and accuracy. The accuracy and precision of these experiments are improved if 9
performed using individual capillary tubes, a method enabling full automation of the measurement. We 10
provide here a protocol to set up and perform these experiments as well as a robust method to measure 11
peptide concentrations using tryptophan as an internal standard. 12

Key words Affinity measurements, Protein–peptide interactions, NMR, Equilibrium binding 13
constants 14

1 Introduction 15

Nuclear Magnetic Resonance (NMR) provides a powerful tool to 16
study protein–ligand and protein–protein interactions at atomic 17
resolution [1]. Among many other possibilities, NMR can be 18
used to measure very accurately the equilibrium constant of the 19
interaction, provided that its equilibrium dissociation constants 20
(K_d) is in the range of 10 μ M or above, a value that corresponds 21
to the study of rather weak interactions. Several methods have been 22
developed to measure protein–ligand dissociation constants, and 23
they are usually classified in two main classes: the “ligand- 24
observed” and the “protein-observed” methods. While “ligand- 25
observed” methods, such as Saturation Transfer Difference (STD) 26
or WaterLogsy share common principles with other biophysical 27
approaches, the “protein-observed” approach is unique to NMR 28
for its ability to deliver site-specific information [2, 3]. Thanks to 29
these properties, NMR is now an established tool in pharmaceutical 30
industry where it is used in drug discovery strategies, essentially at 31

the hit-to-lead step, where low to medium affinity ligands are gradually optimized into potent ligands [4]. The classical approach to study ligand–protein interactions relies on the measurement of protein chemical shift perturbations (CSP) induced by the binding of the ligand. This is generally performed using proteins that are enriched with magnetically active isotopes such as nitrogen 15 or carbon 13 and the prior knowledge of the protein resonance assignments that links a measured nucleus frequency to the corresponding molecular site. The chemical shift perturbations are then monitored using heteronuclear correlation spectra upon successive addition of increasing amounts of ligand. This approach is applicable to very large protein complexes such as the proteasome or the nucleosome, provided that appropriate labeling strategies are used such as the selective labeling of methyl groups [5]. It has been recently shown that this approach is also applicable with non-labeled protein samples thanks to the latest progress in NMR spectrometer sensitivity and the use of relaxation optimized pulse sequences such as Methyl SOFAST [6]. For proteins with molecular weights of less than 20 KDa, the common approach relies on the cost-effective production of ^{15}N labeled samples and the use of highly sensitive ^1H – ^{15}N HSQC correlation spectra to monitor CSP. Here, we present a protocol enabling the equilibrium dissociation constants between a binding peptide and a small protein to be measured with high precision and accuracy. The method relies on the use of several low-volume samples, an approach that provides better accuracy when compared to the classical sequential titration method [7]. The protocol takes advantage of the ability to quantify precisely the amount of ligand present in the different samples as an accurate knowledge of the active concentrations of the interacting partners determines the reliability of the final result. The practical aspects of these measurements are illustrated using the interaction between the third SH3 domain of Vinexin β and a model proline peptide from the N-terminal domain (NTD) of the Retinoic Acid Receptor γ (RAR γ) as a prototypal case (Fig. 1). In this particular study, both accurate and precise measurements of K_d values for different peptides are needed to understand the molecular basis of the affinity modulation by the phosphorylation of the RAR γ NTD [8].

2 Materials

2.1 Protein Production

The protein is obtained using heterologous expression in *E coli* according a protocol that depends on the system under study. Produce 4–5 mg of purified ^{15}N labeled protein using adapted expression and a purification protocols (*see Note 1*).

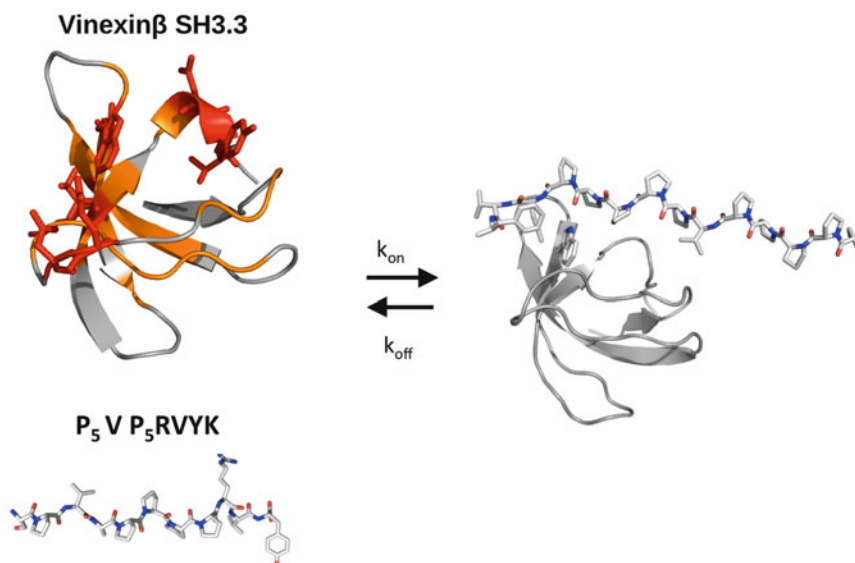


Fig. 1 The titration protocol presented here is illustrated with data originating from an interaction study between a model peptide from the proline-rich region of the RAR γ NTD and the third SH3 domain of the human Vinexin β [8]. The residues highlighted in orange and red show Chemical Shift Perturbation (CSP) of their ^1H - ^{15}N correlation peaks upon addition of increasing amounts of peptide, indicating the location of the binding site on the protein surface. The CSP of *red highlighted* residues that were used to fit the equilibrium dissociation constant K_d

2.2 Peptide Synthesis

Peptides are obtained from the peptide synthesis platform at IGBMC using an ABI 443A synthesizer adapted to Fmoc chemistry. Purify the crude peptide products by reverse phase high performance liquid chromatography (HPLC) before undergoing a second chromatographic purification step in a migration column containing a cluster of resin balls (stable phase). Check the purity (95 % or better) of the resulting product by examining the HPLC elution profile, and by analyzing the peptide by mass spectrometry and NMR (*see Note 1*).

2.3 Capillary System

Use 1.7 mm outer-diameter capillary system for NMR measurements. This system is composed of 75 mm long capillaries capped with a teflon tube which is placed into a sample holder. Use a sample volume of 50 μL , which produces a filling height of 40 mm that was tested to be sufficient. The sample holders have a standard 5 mm outer diameter upper section with a transition to a 3 mm outer diameter (60 mm long) stem. The sample holder is reusable and fits all conventional 5 mm rotors. Fill the space between the capillary and the sample holder with 50 μL of D_2O (deuterated water) for the external lock. The system was purchased from "New-Era" (Vineland, NJ, USA).

[AU2](#)

**2.4 NMR
Measurements**

The NMR measurements should be performed using a high-field (above 600 MHz) NMR spectrometer equipped with a triple resonance cryogenic probe. Set the acquisition parameters to keep the measurement time within reasonable limits of 1–2 h per titration point. If available, use a sample changer to run the experiment unattended overnight (*see Note 2*).

**2.5 Theoretical
Aspects of K_d
Measurements from
NMR Frequencies**

The binding of a ligand peptide (L) to a protein (P) to form a peptide–protein complex (PL) is described by the following equilibrium:



The dissociation equilibrium constant K_d is defined as:

$$K_d = \frac{k_{\text{off}}}{k_{\text{on}}} = \frac{[P][L]}{[PL]} \quad (2)$$

Where $[P]$, $[L]$ and $[PL]$ are the concentrations of the free protein, the free ligand and the complex respectively and k_{on} and k_{off} the association and dissociation rates respectively. The ability to determine the value of the dissociation constant from chemical shift measurements depends on the exchange kinetic between free and bound species, defined as:

$$k_{\text{exc}} = k_{\text{off}} + k_{\text{on}}[L] \quad (3)$$

For k_{exc} values significantly larger than the NMR frequency difference $2\pi(\nu_i^{\text{bound}} - \nu_i^{\text{free}})$ between the bound and free states of the protein, the observed frequency, ν_i is a weighted average between the frequencies of the free and bound states:

$$\nu_i = x_1 \nu_i^{\text{bound}} + (1 - x_i) \nu_i^{\text{free}} \quad (4)$$

$x_i \in [0, 1]$ is the occupancy of a given binding site i within the protein. This averaging situation occurs when k_{off} is rather fast, which corresponds to ligands of weak affinity (in the micromolar to millimolar range). Assuming that the frequency change of a given nucleus within the protein is essentially due to local perturbations, its value provides therefore a direct measurement of the occupancy of the binding site localized in its vicinity using:

$$x_i = \frac{\nu_i - \nu_i^{\text{free}}}{\nu_i^{\text{bound}} - \nu_i^{\text{free}}} \quad (5)$$

The subscript i highlights the unique ability of NMR spectroscopy to measure site-specific affinity binding constants. The value of the site-specific dissociation constant, K_d^i , is subsequently obtained using a nonlinear fit of the following equation:

$$x_i^2 - x_i \left(1 + \frac{[L]_0}{[P]_0} + \frac{K_d^i}{[P]_0} \right) + \frac{[L]_0}{[P]_0} = 0 \quad (6)$$

with: $[L_0] = [L] + [PL]$ and $[P_0] = [P] + [PL]$ 130

K_d^i and ν_i^{bound} are adjustable parameters to minimize the value 131
of the target function: 132

$$f(K_d^i, \nu_i^{\text{bound}}) = \frac{1}{N} \sum_{j=1}^N \left(\nu_{i,j}^{\text{calc}} - \nu_{i,j}^{\text{obs}} \right)^2 \quad (7)$$

$\nu_{i,j}^{\text{calc}}$ is a frequency calculated for a given total concentrations of 133
protein $[P]_{0,j}$ and ligand $[L]_{0,j}$, using equations (Eqs. 4 and 6) 134
while $\nu_{i,j}^{\text{obs}}$ is the corresponding measured frequency. The subscript 135
 j identifies each single titration point from the total number of N 136
different mixtures of protein and ligand. 137

The protein frequencies are usually measured using ^{15}N or ^{13}C 138
labeled proteins and heteronuclear correlation spectra. For small 139
proteins, such as a SH3 domain, ^1H - ^{15}N correlation spectra provide 140
an inexpensive and accurate way to monitor the chemical shift 141
perturbations induced by the binding of a ligand. Both nitrogen 142
and its bound amide proton frequencies are reported using a composite 143
chemical shift (frequency) usually defined as: 144

$$\delta_{\text{comp}} = \sqrt{\delta_{^{15}\text{N}}^2 + \left(\frac{\gamma_{\text{H}}}{\gamma_{\text{N}}} \delta_{^1\text{H}} \right)^2} \quad (8)$$

145

3 Methods

146

3.1 Design of the NMR Titration Experiment

1. The feasibility of the affinity measurement by NMR will depend 147
on the K_d value and the ability to get the protein and the 148
peptide at concentrations that are compatible with NMR mea- 149
surements. The minimal protein concentration required to 150
acquire ^1H - ^{15}N heteronuclear correlation spectra varies 151
between 10 and 100 μM , depending on the available NMR 152
spectrometer. Check with classical methods (UV, DLS, ...) 153
whether the protein of interest can be concentrated up to 154
these values using a non-labeled protein sample. 155
2. Check the quality of the ^{15}N labeled sample by recording a 156
 ^1H - ^{15}N HSQC spectrum of your stock protein solution at 157
its highest concentration. Standard large volume NMR tubes 158
(5 or 3 mm tubes) can be used for this purpose. Check the 159
stability of the protein sample at the planned measurement 160
temperature by recording a ^1H - ^{15}N HSQC spectrum after a 161
few days at this temperature. The appearance of a subset of 162
sharp peaks is indicative of protein degradation (*see Note 3*). 163

3. Desalt the peptide and transfer it to the buffer used for the protein. Both steps could be done at once using a gel filtration column such as the Superdex Peptide 10/300 GL (*see Note 4*).
4. Since the method presented here is only applicable when the protein–peptide interaction leads to a so-called “fast exchange regime,” it is important to check whether this condition holds true for the system of interest at an early stage of the study. This could be done by preparing an initial sample with approximately stoichiometric concentrations of protein and peptide and by recording a ^1H – ^{15}N HSQC spectrum of this sample. Four distinct situations may be encountered:
 - The correlation map of the mixture is identical to the one obtained for the sole protein, indicative of an absence of interaction.
 - The spectrum displays broader correlation peaks and several peaks are missing. This case corresponds to more complex situations where the protein undergoes an intermediate time-scale exchange between two (peptide-bound and free) or more states, preventing K_d measurements.
 - A second set of correlation peaks is observed. This is indicative of a “slow exchange regime” corresponding to tight interactions between the protein and the peptide. No quantitative measurement of the K_d will be possible using chemical shift measurements.
 - The correlation map of the mixture contains the same number of peaks, but several of these peaks have different frequencies when compared to the peptide-free spectrum of the protein. This situation will allow the measurement of the K_d .

3.2 Measurement of Peptide and Protein Concentrations

Several factors do affect the accuracy and precision of equilibrium constant measurements by NMR, the most important one being inaccurate estimations of protein and ligand concentrations (*see Note 5*). While the protein concentration may be measured with reasonable accuracy using its absorption at 280 nm, this is not the case for the peptides, in particular when they lack tryptophan or tyrosine residues. It is therefore essential to ensure an accurate measurement of protein and peptide concentrations. We report hereafter a simple method that provides reasonable accuracy for peptide concentration measurements by NMR (below 10 %) (*see Note 6*).

1. Prepare a stock solution of tryptophan by weighting about 6 mg of L-Tryptophan (MW: 204.23 g/mol). Dissolve the powder in 5 mL of D₂O 99.9 %.

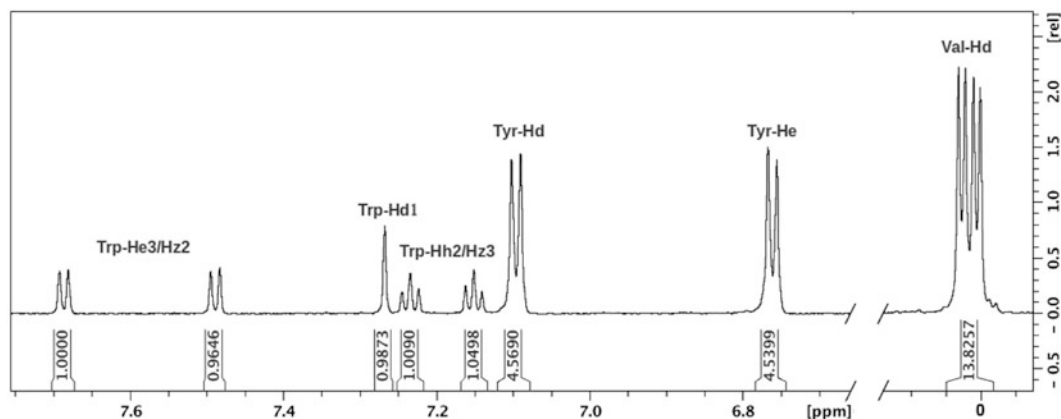


Fig. 2 1D proton spectrum of a mixture between a model peptide (sequence P₅VP₅RVYK) corresponding to the proline-rich region of the RAR γ NTD and the tryptophan solution of known concentration. The amount of peptide required for this concentration measurement was 15–20 μ g. The ratio between the averaged integrals of the tryptophan peaks and those of the peptide indicated that the peptide was 2.3 times more concentrated than the tryptophan. Given the concentration of the tryptophan standard, this led to concentration of 4.5 ± 0.2 mM for the peptide stock solution. The relative uncertainty on the peptide concentration using this method was 4.4 %

2. Measure the concentration of the L-Tryptophan stock solution (5–6 mM) by measuring the absorption at 280 nm ($\epsilon_{280} = 5,690 \text{ mol}^{-1} \cdot \text{cm}^{-1}$) (*see Note 7*).
3. Prepare a NMR sample by mixing a small volume (10–20 μ L) of peptide (whose stock solutions are usually available at millimolar concentration) with (5–20 μ L) of L-Tryptophan stock solution. Complete with D₂O to get a total sample volume of 150–170 μ L, suitable for a 3 mm tube.
4. Record a 1D proton NMR spectrum of the sample with water pre-saturation for solvent signal suppression. Adjust the number of scans to get a reasonable signal-to-noise ratio according the sensitivity of your spectrometer. A long relaxation delay (10–15 s) should be used to account for the long T₁ of the tryptophan aromatic protons (about 3 s) (Fig. 2).
5. Perform a baseline correction and integrate the signals of the tryptophan aromatic protons as well as one or few isolated resonance peaks of the peptide (we often use methyl groups resonances). Compute the ratio between the areas (normalized by the number of protons resonating at the corresponding frequency) measured for the peptide and the tryptophan to get the concentration of the peptide stock solution $[L]_0$ using:

$$[L]_0 = \frac{A_L N_w DF_L}{A_w N_L DF_w} [W]_0 \quad (9)$$

Where A_L is the areas measured under one or several peaks corresponding to N_L proton resonances of the peptide. A_w and

N_w are the corresponding values obtained for the tryptophan resonances. DF_L and DF_w are the dilution factors used to prepare the sample from the peptide and the tryptophan stock solutions, respectively. $[W]_0$ is the concentration of the tryptophan stock solution determined in **step 2**.

6. Measure the protein concentration using its absorption at 280 nm.

3.3 NMR Capillaries Preparation and NMR Acquisition

- Prior the titration experiment, the protein concentration needed to achieve a reasonable signal-to-noise (S/N) ratio on the heteronuclear ^1H - ^{15}N HSQC spectra should be adjusted. On a 700 MHz equipped with a cryoprobe, a protein concentration (the SH3.3 domain of Vinexin β) of 50 to 80 μM in a 1.7 mm capillary tube provides good quality spectra. This will highly depend on the available NMR equipment as well as on the system under study. The use of NMR capillary tubes is of particular interest when titration experiments have to be performed in high salt concentrations (*see Note 8*). As an example, the comparison of relative sensitivity measured on SH3 samples using standard 5 mm, 3 mm tubes and capillary tubes at 700 MHz is provided in Table 1. Despite the apparent reduced signal-to-noise ratio observed for low-volume samples, the relative sensitivity (sensitivity per amount of material) is significantly increased, up to a factor of 3 with capillaries as shown in Table 1 (*see Note 9*).
- Prepare the different protein-peptide mixtures in Eppendorf tubes. Adjust the sample volume according the capacity of the chosen capillaries. For 1.7 mm capillaries, the volume is adjusted to 75 μL using the protein buffer (*see Note 1*). Fill the capillaries using a stretched Pasteur pipette or a Hamilton syringe. Add 50 μL buffer in the capillary holder for external lock. After capping the capillaries, insert them within the capillary holder as shown in Fig. 3. As an example, we provide here a sample preparation table (Table 2) that was used to measure the

t.1 **Table 1**
Experimental sensitivities per amount of protein, relative to a 5 mm (550 μL) NMR tube

AU4

Sample geometry	550 μL 5 mm tube 9 % D_2O in sample	180 μL 3 mm tube 9 % D_2O in sample	50 μL capillary 9 % D_2O in sample	50 μL capillary no D_2O in sample
Ratio of protein material	1	0.33	0.09	0.1
HSQC S/N	763	569	179	241
Relative sensitivity	1	2.26	2.61	3.16

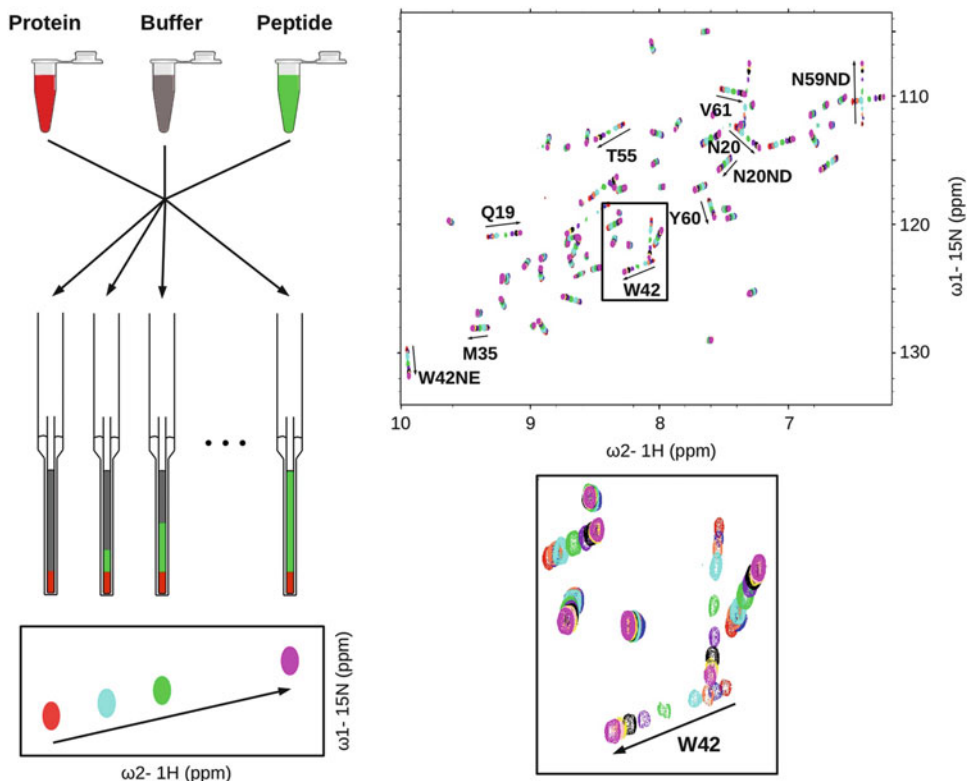


Fig. 3 Preparation of capillary tubes (*left*) for ^1H - ^{15}N HSQC measurements (*right*). The insert shows a close-up on the effect of increasing amounts of peptide on the cross peak corresponding to the backbone amide proton of Tryptophan 42, which is located within the binding site (*see Fig. 1*)

affinity of SH3.3 domain of Vinexin β to a proline rich peptide 267
from the RAR γ NTD (*see Note 10*). 268

3. For each sample, record a ^1H - ^{15}N HSQC heteronuclear spectrum with sufficient acquisition time and resolution to allow a precise measurement of nitrogen and proton frequencies. 269
270
271
4. The processed spectra should be superposed in order to identify the ^1H - ^{15}N correlation peaks that are subjected to the largest frequency shifts upon addition of the peptide. Perform a peak-picking on each spectrum in order to compute a composite chemical shift perturbation using: 272
273
274
275
276

$$\Delta\delta_{\text{comp}} = \sqrt{(\Delta\delta_{\text{N}})^2 + \left(\frac{\gamma_{\text{H}}}{\gamma_{\text{N}}}\Delta\delta_{\text{H}}\right)^2} \quad (10)$$

where $\Delta\delta_{\text{N}}$ and $\Delta\delta_{\text{H}}$ are the difference between the nitrogen and proton chemical shifts measured with a given amount of peptide and those measured in absence of peptide. γ_{H} and γ_{N} are the gyromagnetic ratios of the proton and the nitrogen respectively (*see Notes 11 and 12*). 277
278
279
280
281

t.1 **Table 2**
 Composition of samples used for the titration of the C-terminal SH3 domain of human Vinexin β with the P₅VP₅RVYK peptide

t.2	Sample N°	Conc. Peptide stock (μ M)	Volume SH3 (μ L)	Volume peptide (μ L)	Volume buffer (μ L)	Conc. SH3 (μ M)	Conc. peptide (μ M)	Stoichiometric ratio
t.3	1	45	15	0	60	64.4	0	0
t.4	2	45	15	18	42	64.4	10.8	0.17
t.5	3	450	15	3	57	64.4	18	0.28
t.6	4	450	15	6	54	64.4	36	0.56
t.7	5	450	15	15	55	64.4	90	1.40
t.8	6	4,500	15	3	57	64.4	180	2.80
t.9	7	4,500	15	6	54	64.4	360	5.59
t.10	8	4,500	15	12	48	64.4	720	11.18
t.11	9	4,500	15	16	44	64.4	960	14.91
t.12	10	4,500	15	30	30	64.4	1,800	27.95
t.13	11	4,500	15	50	10	64.4	3,000	46.58

3.4 Data Analysis and Error Estimates

The first step of the analysis consists in estimating the number of peptide binding site on the protein surface. (1) a single binding site and one step binding mechanism are characterized by a linear trajectory of the peak in the ^1H - ^{15}N HSQC series [6, 7, 9]. This should be carefully checked, as the K_d is only defined under these conditions. (2) Further check can be performed by mapping the location of the corresponding amino acids on the protein structure, if both the structure and the HSQC assignment are known (see Note 13). (3) A last insight is provided by the numerical analysis of chemical shift data. The fitting procedure described below may first be applied using individual ^1H - ^{15}N correlations first to extract local K_d values. Their convergence to an identical dissociation constant provides a strong indication that these ^1H - ^{15}N sites monitor the peptide occupancy of the same binding site (see Note 14).

1. Find the values of K_d and $\Delta\delta_{\text{comp}}^{\text{max}}$ that leads to a minimal value of Eq. 8. This could be performed using least-square fitting procedures available in CcpNmr or other protein NMR software packages. We recommend using Python scripts which offers more flexibility in data analysis and plotting (see Note 15). Average the Chemical shift changes of Amide groups that belong to the same binding site in order to increase the precision of the binding site occupancy measurement. In case of the Vinexin β SH3.3 domain, an average chemical shift

perturbation was calculated from 10 ^1H - ^{15}N correlations 306
corresponding to residues Q19, N20, N20ND, M35, W42, 307
W42NE, T55, N59ND, Y60, and V61 (highlighted in Fig. 3). 308

2. Estimate the uncertainty on the resulting K_d values. This is 309
done using a Monte Carlo simulation where synthetic datasets 310
are generated and subsequently fitted. These synthetic datasets 311
are generated using a Gaussian distribution of $\Delta\delta_{\text{comp}}$ using 312
the values calculated from the first fit as the mean and the 313
root-mean square deviation (the square root of Eq. 8) as the 314
standard deviation. The uncertainties on protein and peptide 315
concentrations are taken into account by generating distribu- 316
tions of peptide and protein total concentrations around 317
the initial values. The width of the distribution is given by the 318
uncertainties on the concentrations (*see Note 16*). As concen- 319
tration values can't be negative, the Log-normal distribution 320
is chosen to generate the distribution of concentration 321
values [10]. The distribution width is then directly given by 322
the relative uncertainties on the measured concentrations 323
(*see Notes 17 and Note 18*). 324

325

4 Notes

326

1. The protocol used to purify the C-terminal SH3.3 domain of 327
human Vinexin β (REFSEQ: NP 001018003) was a classical 328
two steps purification protocol (Glutathione affinity and gel 329
filtration) that is described in ref. 8. Alternatively, ^{13}C , ^{15}N 330
double-labeled proteins are also suitable for titration experi- 331
ments. The final buffer was a low salt phosphate buffer with 332
20 mM sodium phosphate at pH 7.0, 100 mM NaCl. 333
2. We used a BRUKER Avance III 700 MHz spectrometer 334
equipped with a TCI cryoprobe and a BACS60 sample changer. 335
 ^1H - ^{15}N -HSQC spectra were recorded with 32 scans and 128 336
data points in the indirect dimension resulting in a total acqui- 337
sition time of 90 min per sample. 338
3. Several precautions may be used to prevent, or at least slow 339
down protein degradation. Antiproteases are usually added to 340
the final sample as well as sodium azide (NaN_3) (0.01 % w/v) 341
used as an antibacterial. If the protein sequence contains free 342
cysteines, we usually add reducing agents such as Dithiothreitol 343
(DTT) or TCEP (Tris(2-carboxyethyl)phosphine). In that case, 344
all used buffers should be carefully degassed and oxygen 345
removed from the sample by Helium or Argon bubbling. 346
4. Protocols used for peptide synthesis and purification lead to the 347
presence of significant amount of trifluoro acetic acid (TFA) 348
salts in dry peptide samples. NMR provides an accurate method 349

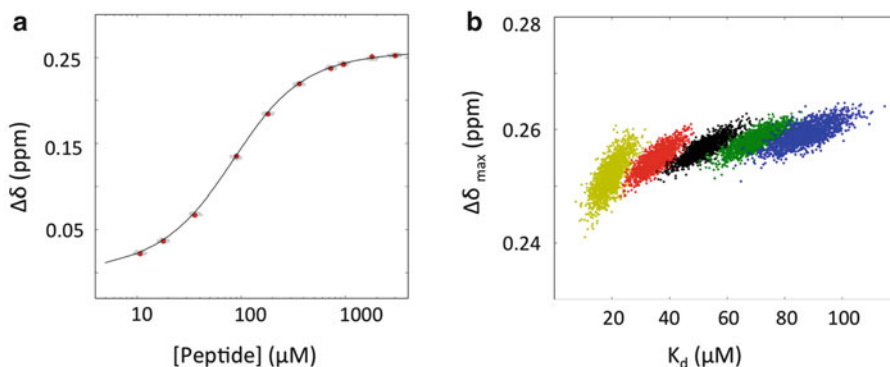


Fig. 4 Least-square fit of the chemical shifts perturbation data measured for the interaction between the P₅VP₅R_VYK model peptide and the Vinexin β SH3.3 domain. **(a)** Semi-log plot of the composite chemical shifts computed from ten residues of SH3.3 as a function of peptide concentrations. Pseudo experimental points generated for the Monte Carlo estimate of the uncertainty on the K_d value are shown in *gray*. These points are distributed according to a gaussian distribution for the $\Delta\delta$ values and according to a log-normal distribution for the peptide and protein concentrations. **(b)** Distribution of the two fitted parameters after the Monte Carlo procedure. The concentration uncertainties were estimated to be 10 % for the SH3.3 protein and between 4 and 5 % for the peptide. The calculations were performed for a peptide stock solution whose concentration was either underestimated by a factor of 0.6 and 0.8 (*yellow* and *red*), or overestimated by 1.2 and 1.4 (*green* and *blue*). The *black* points reflect the effect of pure random noise of the fitting procedure as the concentration of peptide stock solution is considered to be accurate

to check both the efficiency of the desalting procedure and 350
the purity of the final peptide solution by recording ^1H and ^{19}F 351
1D spectra of the stock peptide solution. Depending on the 352
peptide sequence, we found that the gel filtration desalting 353
method may leave significant amounts of residual trifluoroacetate 354
salts in the final sample. In this case, more efficient protocols 355
should be considered [11]. 356

5. Over or underestimated values of the peptide stock concentra- 357
tion have a dramatic impact on the K_d values resulting from the 358
fit of Eq. 8. This effect can be evaluated by performing Monte 359
Carlo simulations with systematically biased values of ligand 360
concentrations (20 or 40 % above or below the true value, as 361
shown in Fig. 4 and Table 3). The results obtained indicate that 362
a concentration of ligand peptide that is underestimated by 363
30 % leads to an overestimation of the affinity by a factor of 364
30 % (The apparent K_d value is 36 μM instead of 52 μM). This 365
large effect is due to the high correlation that exists between the 366
different measurement points since the corresponding pro- 367
tein-peptide mixtures are usually prepared from the same pep- 368
tide stock solution. 369
6. A method has been recently proposed to compute the molar 370
absorptivity of a protein or peptide at 205 nm from its amino 371
acid sequence, providing an alternative for quantifying peptides 372

Table 3

Average values and standard deviations of dissociation constants (K_d) and chemical shift perturbations ($\Delta\delta_{\max}$) values computed from Monte Carlo calculations

	Relative uncertainties (one standard deviation) on peptide concentrations				
	10 %	20 %	30 %	40 %	50 %
K_d (μM)	52.3 ± 5.6	52.0 ± 9.9	52.5 ± 14.6	53.9 ± 19.8	52.3 ± 22.3
$\Delta\delta_{\max}$ (ppm)	0.257 ± 0.002	0.256 ± 0.003	0.256 ± 0.005	0.256 ± 0.006	0.255 ± 0.007

	Ratio between measured and real peptide concentrations				
	0.6	0.8	1.	1.2	1.4
K_d (μM)	19.6 ± 3.8	35.6 ± 4.2	52.1 ± 5.4	69.8 ± 6.1	87.4 ± 7.3
$\Delta\delta_{\max}$ (ppm)	0.252 ± 0.003	0.255 ± 0.002	0.257 ± 0.002	0.258 ± 0.002	0.259 ± 0.002

Experimental chemical shifts were obtained from the interaction of the P₅VP₅RVYK peptide with the Vinexin β SH3.3 domain. The uncertainty of the SH3.3 protein concentration was estimated to be 10 %. The fitted values are reported for different uncertainties of the peptide concentrations (*upper panel*) or for a systematic error on peptide stock solution (*lower panel*).

lacking tryptophan or tyrosine residues [12]. Combining this measurement with the quantitative evaluation of peptide concentration by NMR provides an interesting way to get robust estimates of concentrations. Other methods have been proposed for protein concentrations measurements by NMR, such as PULCON for instance [13].

7. In order to increase the precision of this OD measurement, we usually perform several OD_{280 nm} measurements with targeted absorption values of 0.8, 0.4, 0.2, and 0.1. The linear regression of this series of measurements is used to provide an estimation of the uncertainty on the Tryptophan stock solution concentration.

8. The Signal-to-Noise ratio (S/N) in NMR may be written as:

$$S/N \propto \frac{M_0 B_1}{\sqrt{P_s(T_a + T_s) + P_c(T_a + T_c)}} \quad (11)$$

where M_0 is the spin magnetization, B_1 the radio-frequency (RF) field intensity applied to the sample, and P_c and P_s are the RF power absorbed by the coil and by the sample, respectively. T_c and T_s are the temperature of the coil and the sample, respectively, while T_a is the noise temperature of the preamplifier [14–16]. Recent progress in NMR probe development, most notably the development of cryogenic probes, improved the S/N by lowering T_c and T_a down to 10–25 K and by reducing P_c by optimizing the coil quality factor (*see ref. 16*).

There remains room for S/N optimization on the P_s term, which is mostly dependent on the sample itself because of dielectric losses. It is known that the RF power dissipated in the sample depends on the dielectric constant of the medium which is very much dependent on the type of solvent and on the ionic strength when working in H_2O . Thus, the P_s term depends on the distribution of the electric field within the sample geometry and on the strength of the RF irradiation (expressed as its angular frequency ω_1) with:

$$P_s \propto \omega_1^2 \quad (12)$$

Because of this dependency, P_s losses become more prominent with increasing fields. On a given probe, reducing the internal diameter of the NMR tube with a capillary system has two opposite effects on the overall sensitivity of the measurement. First, reducing the sample volume at a given concentration results in a loss of signal due to a proportional reduction of sample quantity. However, the power dissipated within the sample P_s is also reduced and so is the noise, leading to a potential improvement of the S/N. The balance between these two effects strongly depends on the nature of the sample itself, and the amount of the overall effect is not directly predictable. Finally, it should be mentioned that the use of capillary tubes centers the sample in the inner volume of the coil where the electric field is minimum and the impact on P_s and thus on the noise is maximum. This effect has been studied [17] and it was shown that in high salt conditions it is actually beneficial in terms of S/N to reduce the NMR tube diameter while keeping all concentrations constant.

9. This gain results from several factors. First, the signal noise arising from RF losses in the sample itself is minimized in small diameter tubes due to a lower value of P_s , the RF power dissipated within the sample (*see Note 8*). This effect will be of increasing importance if high salt concentrations are required for the protein buffer and if a cryogenically cooled probe is used. A second source of sensitivity gain originates from a more optimal use of the sample volume as only about 30 % of the sample volume is outside the RF coil. On 5 mm tubes, susceptibility matched NMR tubes or plugs (Shigemi tubes) are usually used to compensate this effect, allowing doubling the relative sensitivity. Though the handling of these systems is cumbersome, the susceptibility matched approach can also be applied on capillary tubes, with a potential further 43 % gain in relative sensitivity. Finally, the use of an external lock implies that there is no need to add deuterium into the sample itself which otherwise leads to an additional loss of signal due to deuterium exchange of the amide protons. Notably, the

- capillary sample lacking 9 % D2O enables another 21 % of gain 440
in relative sensitivity. 441
10. In our example, the concentration of the protein is constant 442
while the peptide concentration varies. It has been shown that 443
an optimal sampling is achieved when both the protein and 444
peptide concentrations are varied together [18]. 445
 11. Peak picking is usually performed using the software packages 446
dedicated to protein NMR spectra analysis such as SPARKY 447
(<http://www.cgl.ucsf.edu/home/sparky>), CcpNmr Analysis 448
(<http://www.ccpn.ac.uk>) or CARA (<http://cara.nmr.ch>). 449
Peak tracking can be performed with algorithms such as 450
described in [19] for instance. 451
 12. The ratio γ_H/γ_N is a weighting factor that compensates the 452
difference of chemical shift ranges between proton and nitro- 453
gen frequencies. Its precise value is of little importance and 454
there are also other weighting factors described in the 455
literature. 456
 13. The resonance assignment of a variety of proteins can be 457
obtained from the Biological Magnetic Resonance Data Base 458
(BMRB) at <http://www.bmrb.wisc.edu/>. 459
 14. The knowledge of the resonance assignments is not required to 460
identify two binding sites if their affinity are different and if this 461
difference could be resolved by NMR titration experiments as 462
shown in [6]. 463
 15. The set of Python script used to analyze the interaction 464
between the Vinexin β SH3.3 domain and the P₅VP₅RVYK 465
RAR γ model peptide is available at <http://zenodo.org> (doi: 466
[10.5281/zenodo.11663](https://doi.org/10.5281/zenodo.11663)). 467
 16. The propagation of uncertainties of volume measurements 468
follows the general law: 469

$$u^2(y) = \sum_{i=1}^N \left(\frac{\partial f}{\partial x_i} \right)^2 u^2(x_i) + 2 \sum_{i=1}^{N-1} \sum_{j=i+1}^N \frac{\partial f}{\partial x_i} \frac{\partial f}{\partial x_j} \text{cov}(x_i, x_j)$$

(13)

where $u(y)$ is the uncertainty on the concentration that depends 470
on several variables ($y = f(x_i)$) depending on the specific 471
scheme that is used for sample preparation. The covariance 472
($y = f(x_i)$) was set to 1 for volumes if the same pipette was 473
used twice, and for concentrations when the same solution was 474
used. The calculation of uncertainty propagation used for the 475
Vinexin β work is available at the following address: [http://](http://zenodo.org) 476
[zenodo.org](https://doi.org/10.5281/zenodo.11663) (doi: [10.5281/zenodo.11663](https://doi.org/10.5281/zenodo.11663)). 477

17. Two main types of uncertainties have to be distinguished: an 478
erroneous estimation of the peptide stock solution will lead to a 479

t.1 **Table 4**
 t.2 **Comparison of the uncertainties on ligand concentrations for sequential or**
 t.3 **parallel titration experiments**

		Absolute (μM) and relative ligand concentration uncertainties	
	Sample number	Peptide concentration (μM)	
			Sequential titration scheme Parallel titration scheme
t.4	0	0.0	
t.5	1	10.8	4.8 % (0.52) 4.9 % (0.53)
t.6	2	18.0	3.7 % (0.66) 4.9 % (0.89)
t.7	3	36.0	4.1 % (1.49) 4.8 % (1.74)
t.8	4	90.0	5.4 % (4.84) 4.8 % (4.28)
t.9	5	180.0	5.8 % (10.5) 4.8 % (8.66)
t.10	6	360.0	6.7 % (24.3) 4.7 % (16.9)
t.11	7	720.0	7.4 % (53.5) 4.6 % (33.3)
t.12	8	960.0	6.4 % (61.9) 4.6 % (44.3)
t.13	9	1800.0	7.0 % (126.3) 4.6 % (82.7)
t.14	10	3000.0	5.1 % (152.7) 4.5 % (135.4)
t.15		Max uncertainty:	7.4 % 4.9 %

systematic bias in the resulting K_d values, while pipetting errors will introduce random noise on the measurements. We have simulated both effects and the resulting uncertainties on fitted parameters are shown in Table 3. While a random noise of 20 % on the peptide concentration leads to a resulting relative uncertainty of 20 % on the K_d value, a 20 % underestimation of the peptide concentration leads to overestimation of the affinity by more than 30 % (36 μM instead of 52 μM). This emphasizes the importance of having the most accurate peptide concentration values before undertaking affinity measurements by NMR or by any other methods.

18. In order to provide a quantitative estimation of these effects, we performed formal calculations to compute the uncertainties on the protein and peptide concentrations for each point of the titration that arise from the uncertainties of volume measurements. These later values were taken from the specifications provided by the pipette manufacturer (Gilson Inc.). The resulting absolute and relative uncertainties on the ligand concentrations together with their impact on the resulting K_d are reported in Table 4. The parallel titration protocol leads to

maximal relative error on ligand concentrations of 4.9 %, a value that is lower than the one obtained (7.4 %) if the experiment would have been performed using a regular sequential addition of ligand to the same tube. It is worth noting that this calculation is probably underestimating the uncertainty associated with the sequential titration protocol as the multiple manipulations of the same tube will lead to unavoidable losses of sample volume, in particular when susceptibility matching tubes are used.

Acknowledgments

509

This work was supported by the ANR program VINRAR ANR-09-BLAN-0297, the Institut National du Cancer [grant number INCa-PL09-194], the Ligue Regional contre le cancer and by the French Infrastructure for Integrated Structural Biology (FRISBI) ANR-10-INSB-05-01, as part of the European Strategy Forum on Research Infrastructures (ESFRI) and through national members agreements. The authors thank Claude Ling (IGBMC) for technical support, the chemical peptide synthesis service at IGBMC and Yves Nominé for critical reading of the manuscript.

517
518

References

- [AU7](#) 519
[AU8](#) 520
- 522 1. Kieffer B, Homans S, Jahnke W (2011) Nuclear magnetic resonance of ligand binding to proteins. In: Podjarni A, Dejaegere A, Kieffer B (eds) Biophysical approaches determining ligand binding to biomolecular targets. RSC, Cambridge, UK, pp 15–55 549
 - 523 2. Fielding L (2007) NMR methods for the determination of protein–ligand dissociation constants. *Prog Nucl Magn Reson Spectrosc* 51:219–242 550
 - 524 3. Dalvit C (2009) NMR methods in fragment screening: theory and a comparison with other biophysical techniques. *Drug Discov Today* 14:1051–1057 551
 - 525 4. Pellecchia M, Bertini I, Cowburn D, Dalvit C, Giralt E, Jahnke W, James TL, Homans SW, Kessler H, Luchinat C, Meyer B, Oschkinat H, Peng J, Schwalbe H, Siegal G (2008) Perspectives on NMR in drug discovery: a technique comes of age. *Nat Rev Drug Discov* 7:738–745 552
 - 526 5. Sprangers R, Kay LE (2007) Quantitative dynamics and binding studies of the 20S proteasome by NMR. *Nature* 445:618–622 553
 - 527 6. Quinternet M, Starck JP, Delsuc MA, Kieffer B (2012) Unraveling complex small-molecule binding mechanisms by using simple NMR spectroscopy. *Chem Eur J* 18:3969–3974 554
 - 528 7. Bourry D, Sinnaeve D, Gheysen K, Fritzinger B, Vandenborre G, Van Damme EJ, Wieruszkeski JM, Lippens G, Ampe C, Martins JC (2011) Intermolecular interaction studies using small volumes. *Magn Reson Chem* 49:9–15 555
 - 529 8. Laveve S, Bour G, Quinternet M, Samarut E, Kessler P, Vitorino M, Bruck N, Delsuc MA, Vonesch JL, Kieffer B, Rochette-Egly C (2010) Vinexin β , an atypical “sensor” of retinoic acid receptor gamma signaling: union and sequestration, separation, and phosphorylation. *FASEB J* 24:4523–4534 [AU9](#) 556
 - 530 9. Williamson MP (2013) Using chemical shift perturbation to characterise ligand binding. *Prog Nucl Magn Reson Spectrosc* 73:1–16 557
 - 531 10. Limpert E, Stahel WA, Abbt M (2001) Log-normal distributions across sciences: keys and clues. *Bioscience* 51:341–352 558
 - 532 11. Roux S, Zekri E, Rousseau B, Paternostre M, Cintrat JC, Fay N (2008) Elimination and exchange of trifluoroacetate counter-ion from cationic peptides: a critical evaluation of different approaches. *J Pept Sci* 14:354–359 559

- 574 12. Anthis NJ, Clore GM (2013) Sequence-
575 specific determination of protein and peptide
576 concentrations by absorbance at 205 nm. *Pro-*
577 *tein Sci* 22:851–858
- 578 13. Wider G, Dreier L (2006) Measuring protein
579 concentrations by NMR spectroscopy. *J Am*
580 *Chem Soc* 128:2571–2576
- 581 14. Hoult DI, Lauterbur PC (1979) The sensitivity
582 of the zeugmatographic experiment involving
583 human samples. *J Magn Reson* 34:425–433
- 584 15. Hoult DI (1996) Sensitivity of the NMR
585 experiment. In: Grant DM (ed) *Encyclopaedia*
586 *of nuclear magnetic resonance*. Wiley, New
587 *York, NY*
- 588 16. de Swiet TM (2005) Optimal electric fields for
589 different sample shapes in high resolution NMR
590 spectroscopy. *J Magn Reson* 174:331–334
17. Voehler MW, Collier G, Young JK, Stone MP,
Germann MW (2006) Performance of cryo-
genic probes as a function of ionic strength
and sample tube geometry. *J Magn Reson*
183:102–109
18. Markin CJ, Spyropoulos L (2012) Increased
precision for analysis of protein-ligand
dissociation constants determined from
chemical shift titrations. *J Biomol NMR*
53:125–138
19. Ravel P, Kister G, Malliavin TE, Delsuc MA
(2007) A general algorithm for peak-tracking
in multi-dimensional NMR experiments. *J Bio-*
mol NMR 37:265–275
20. Kovrigin EL (2012) NMR line shapes and
multi-state binding equilibria. *J Biomol NMR*
53:257–270

Uncorrected Proof

Author Queries

Chapter No.: 22 317550_3_En

Query Refs.	Details Required	Author's response
AU1	Please check whether the affiliations of the authors are presented appropriately.	
AU2	Please check whether the edited value in the sentence "1.7 mm outer-diameter capillary system..." is appropriate.	
AU3	Please check whether the values (bold, italic) are presented appropriately throughout the chapter (both in equations and text).	
AU4	Please provide the significance for "bold emphasis" given in the Table 1.	
AU5	The list starting with "Find the values of Kd and..." has been renumbered. Please check.	
AU6	Please check whether the footer presented in Table 3 is appropriate.	
AU7	Note that reference [20] (original [8]) is not cited in text. Please cite the reference in text or delete it from the list.	
AU8	Note that refs. 2b, 6b, and 11b has been renumbered and cited sequentially in text. Please check whether the cross references are appropriate.	
AU9	Please check whether the article title in ref. [8], is presented appropriately.	